MECHANISTIC STUDIES ON THE RADIOLYTIC DECOMPOSITION OF PERCHLORATES ON THE MARTIAN SURFACE

Andrew M. Turner[1,2], Matthew J. Abplanalp[1,2], and Ralf I. Kaiser[1,2]
[1] Department of Chemistry, University of Hawaii at Manoa, Honolulu, HI 96822, USA
[2] W. M. Keck Laboratory in Astrochemistry, University of Hawaii at Manoa, Honolulu, HI 96822, USA

ABSTRACT

Perchlorates—inorganic compounds carrying the perchlorate ion (ClO_4^-)—were discovered at the north polar landing site of the Phoenix spacecraft and at the southern equatorial landing site of the Curiosity Rover within the Martian soil at levels of 0.4–0.6 wt%. This study explores in laboratory experiments the temperature-dependent decomposition mechanisms of hydrated perchlorates—namely magnesium perchlorate hexahydrate ($Mg(ClO_4)_2 \cdot 6H_2O$) —and provides yields of the oxygen-bearing species formed in these processes at Mars-relevant surface temperatures from 165 to 310 K in the presence of galactic cosmic-ray particles (GCRs). Our experiments reveal that the response of the perchlorates to the energetic electrons is dictated by the destruction of the perchlorate ion (ClO_4^-) and the inherent formation of chlorates (ClO_3^-) plus atomic oxygen (O). Isotopic substitution experiments reveal that the oxygen is released solely from the perchlorate ion and not from the water of hydration (H_2O). As the mass spectrometer detects only molecular oxygen (O_2) and no atomic oxygen (O), atomic oxygen recombines to molecular oxygen within the perchlorates, with the overall yield of molecular oxygen increasing as the temperature drops from 260 to 160 K. Absolute destruction rates and formation yields of oxygen are provided for the planetary modeling community.

Key words: astrochemistry – methods: laboratory: solid state – molecular processes – planets and satellites: surfaces – planets and satellites: terrestrial planets

1. INTRODUCTION

Perchlorates—inorganic compounds carrying the perchlorate ion (ClO_4^-)—were discovered at the north polar landing site of the Phoenix spacecraft (Hecht et al. 2009; Kounaves et al. 2010, 2014b) and more recently at the southern equatorial landing site of the Curiosity Rover (Sutter et al. 2013; Archer et al. 2014) within the Martian soil at levels of 0.4–0.6 wt% (Smith et al. 2014). Evidence of Martian perchlorates was also found in the Mars meteorite EETA 79001 (Kounaves et al. 2014a). Further, the evolved gas analysis (EGA) and gas chromatograph mass spectrometer (GC-MS) experiments on the Sample Analysis at Mars (SAM) instrument in the Mars Science Laboratory (MSL) Rover exposed the presence of hydrated perchlorates at the Rocknest deposit in Gale Crater in the equatorial region of Mars (Glavin et al. 2013; Archer et al. 2014; Ming et al. 2014).

An experimental investigation of the degradation products and decomposition mechanisms of perchlorates on the Martian surface by ionizing radiation is of fundamental importance since perchlorates have been attributed to the destruction of organics in the presence of ionizing radiation on Mars (Ming et al. 2009; Navarro-González et al. 2010). A widely accepted hypothesis and one of the main driving forces in Mars exploration is the search for organics—indigenous or external. Indigenous organics include those produced by biology or geology. External organic material is delivered to Mars via meteorites (Marcus 1968; Hartmann 1977; Werner 2008) and interplanetary dust particles (IDPs) at rates of about 10^8 g organic material per year (Hayatsu & Anders 1981; Flynn 1996; Flynn et al. 1997). In particular, Mars should have an annual influx of about 15 ng of amino acids per m^2 per year, which should yield detectable concentrations over a relatively short (geological) time period of 100 years (Ten Kate et al. 2005). The chemical composition of recovered carbonaceous meteorites studied thus far has shown that the majority of the carbon is present as a polyaromatic kerogen-like matrix (Quirico et al. 2005) and a small but significant amount as biorelevant organics such as alcohols (Jungclaus et al. 1976), amino acids (Oró et al. 1971; Pering & Ponnamperuma 1971; Bada 2009), nucleobases (Peeters et al. 2003; Martins et al. 2008; Callahan et al. 2011), and carboxylic acids (Yuen et al. 1984; Cronin & Chang 1993; Cooper & Cronin 1995). As a consequence of the thin atmosphere on Mars, a significant amount of material of 10^3–10^5 meteorites greater than $10 \, g \, km^{-2}$ should land on Mars *without* being oxidized; consequently, intact carbonaceous chondrites may hold a record of organics as these compounds are shielded from UV radiation (Bland & Smith 2000). Considering that the compounds identified within the Murchison meteorite should have been detected with the methods developed for the Viking landings, the lack of organics on Mars was surprising (Biemann 1979). The general consensus is that organic compounds have not been detected on the surface of Mars either by Viking (Biemann et al. 1976, 1977; Biemann & Lavoie 1979) or by the Phoenix Lander (Sutter et al. 2009; Kounaves et al. 2010). However, *very small quantities* of organics in the form of chlorohydrocarbons with up to six carbon atoms such as chlorobenzene—much less than expected based on meteoritic impact—have recently been detected by the Curiosity Rover (Freissinet et al. 2015). Once again, the most widely accepted explanation for this lack of abundant organics is the presence of inorganic oxidants such as perchlorates in the Martian soil (McKay et al. 1998; Glavin et al. 2013; Freissinet et al. 2015).

Laboratory simulation experiments have provided compelling evidence that even complex organic molecules such as glycine (Oró & Holzer 1979; Ten Kate et al. 2006; Noblet et al. 2012), carboxylic acids (Stalport et al. 2009), and naphthalene along with higher mass polycyclic aromatic hydrocarbons (PAHs) (Pang et al. 1982; Hintze et al. 2010) can be degraded

via ionizing radiation in the form of ultraviolet photons and galactic cosmic-ray particles on the surface. However, detailed degradation mechanisms along with the temperature-dependent kinetics of the organics in the presence of perchlorates have been elusive to date, and only limited information on the degradation products (carbon dioxide, smaller hydrocarbons along with their radicals, oxygenated products of the parents) is available. These experiments suggest that the organics could be oxidized by oxygen-containing species such as atomic oxygen (O), the hydroxyl radical (OH), and/or molecular oxygen (O_2), which are released from the (hydrated) perchlorates on the Martian surface upon interaction with ionizing radiation. Therefore, an understanding of the decomposition mechanisms of organics in the presence of perchlorates requires first a quantitative knowledge of the oxygen-containing reactive species that are released by the perchlorates upon exposure to ionizing radiation.

Here, we explore in laboratory experiments the temperature-dependent decomposition mechanisms of hydrated perchlorates—namely magnesium perchlorate hexahydrate ($Mg(ClO_4)_2 \cdot 6H_2O$)—along with the yields of oxygen-bearing species formed in these processes at Mars-relevant surface temperatures from 165 to 310 K in the presence of galactic cosmic-ray particles (GCRs). As a reminder, perchlorates are thought to represent significant oxidants in the soil of Mars with abundances as high as 0.4%–0.6% by weight as detected by the Phoenix Lander (Hecht et al. 2009; Kounaves et al. 2010) and Curiosity Rover (Sutter et al. 2013; Archer et al. 2014). Pavlov et al. demonstrated that due to the lack of a thick atmosphere and intrinsic magnetic field, the surface of Mars is exposed to significant levels of energetic galactic cosmic rays globally (Pavlov et al. 2012). These energetic particles interact with the regolith and also with the perchlorates, causing a cascade of secondary electrons that are available to interact with the Martian soil. Pavlov et al. concluded that Mars receives a dosage of 0.05 J kg^{-1} yr^{-1} of GCR at the surface that can penetrate to a depth of about 2 m in the Martian surface, producing energetic secondary electrons interacting with the surrounding matter—including perchlorates. Our systematic investigations represent the very first step to provide hitherto elusive, but fundamental, information on the initial processes of perchlorate-initiated organic oxidation chemistry in the Martian soil. These findings will bring the planetary science and astrobiology communities to a closer understanding on the chemical evolution and ultimate fate of complex organics on Mars.

2. EXPERIMENT

The experiments were carried out in a contamination-free ultra-high-vacuum (UHV) stainless steel chamber evacuated to a pressure of a few 10^{-10} Torr by exploiting oil-free turbomolecular pumps and dry scroll backing pumps (Bennett et al. 2004). A polished silver mirror positioned in the center of the chamber acts as the substrate and is connected to a rotatable cold finger made out of oxygen-free high-conductivity (OFHC) copper that is interfaced to a two-stage closed-cycle helium compressor (CTI-Cryogenics 1020/9600). Indium foil is placed between the mirror and the cold finger to maximize the thermal conductivity. Individual experiments were carried out at distinct substrate temperatures of 160, 210, and 260 K with an accuracy of ±0.3 K. Note that multiple experiments thus far have shown that the temperature drastically affects the

overall rate of formation of molecules in question during the interaction of ionizing radiation with low-temperature ices (Zheng et al. 2006b; Kim et al. 2010, 2013). At the equator, surface temperatures are in the range from 165 to 310 K, which covers the temperature measurements at the Viking Landers' sites ranging from 166 to 256 K, with 218 K being the average surface temperature. Therefore, our simulation experiments cover the Mars-relevant temperatures.

Samples with an average thickness of 5000 ± 500 nm of magnesium perchlorate hexahydrate ($Mg(ClO_4)_2 \cdot 6H_2O$) were prepared by dissolving 594 mg magnesium perchlorate (Sigma Aldrich, 99%) in 50 ml distilled water (H_2O), adding 0.75 ml of the solutions on the surface of the silver substrate, and evaporating the water between 323 and 333 K. Evaporating at mild temperatures was important to ensure the formation of the hexahydrate complex, and $Mg(ClO_4)_2 \cdot 6H_2O$ was confirmed using infrared spectroscopy. The average thickness can then be calculated from the weight difference of the silver wafer before and after the target preparation (9.0 mg), the area of the silver substrate (9 cm^2), and the density of the sample film (1.98 ± 0.03 g cm^{-3}) (Lewis 1992). Each sample was then irradiated with energetic electrons at 5 keV for 60 minutes with a nominal current of 0 nA (blank experiment) and 100 nA generated by a SPECS EQ 22/35 electron gun, thus exposing the sample to (7.2 ± 0.8) × 10^{14} electrons cm^{-2} over 3.2 ± 0.1 cm^2. After the irradiation, the samples were maintained isothermally for 60 minutes and were then heated to 300 K with a 50 Ω cartridge heater interfaced to the OFHC copper target at 0.5 K minute^{-1}. During the irradiation and in the warm-up phase, the chemical modifications of the samples were probed online and in situ using a Fourier transform infrared (FTIR) spectrometer (Thermo Nicolet 6700) and a quadrupole mass spectrometer (QMS, Pfeiffer Vacuum QMG 422). The FTIR spectrometer collected 196 scans of the irradiated region of the sample for 2 minutes from 6000 to 500 cm^{-1} with a resolution of 4 cm^{-1}; the QMS, operating in the residual gas analyzer mode with an electron impact ionization energy of 90 eV and an emission current of 0.7 mA, detected the subliming species in the gas phase.

The average dose per molecule deposited in the targets was extracted from Monte Carlo simulations accounting for the scattering coefficients and the energy transfer from the electrons to the target (Table 1). For this, the CASINO (v2.42) software (Hovington et al. 1997; Drouin et al. 2007) was exploited to simulate the exposure of magnesium perchlorate hexahydrate ($Mg(ClO_4)_2 \cdot 6H_2O$) with a thickness of 5000 nm and a density of 1.98 ± 0.03 g cm^{-3}. A total of 10^6 trajectories were simulated to mimic the energy transfer processes. These calculations yield average doses of 39 ± 2 eV per formula unit of magnesium perchlorate hexahydrate. Further, the simulation determined the average electron penetration depth to be 235 ± 29 nm, which is much less than the average thickness of 5000 nm. Thus, small variations in the sample thickness due to uneven drying would not affect the results because only the uppermost layers are irradiated.

3. RESULTS

3.1. Infrared Spectroscopy

The infrared spectrum over the range from 2500 to 500 cm^{-1} of the magnesium perchlorate hexahydrate ($Mg(ClO_4)_2 \cdot 6H_2O$)

Table 1
Data Applied to Calculate the Irradiation Dose per Molecule

[a]Initial kinetic energy of the electrons, E_{init}	5 keV
[a]Irradiation current, I	100 ± 2 nA
[b]Total number of electrons	$(2.3 \pm 0.3) \times 10^{15}$
[c]Average kinetic energy of backscattered electrons, E_{bs}	2.9 ± 1.0 keV
[c]Fraction of backscattered electrons, f_{bs}	0.10 ± 0.01
[c]Average kinetic energy of transmitted electrons, E_{trans}	0 keV
[c]Fraction of transmitted electrons, f_{trans}	0
[c]Average penetration depth, l	235 ± 29 nm
[a]Density of the ice, ρ^a	1.98 ± 0.03 g cm^{-3}
[a]Irradiated area, A	3.2 ± 0.1 cm^2
[b]Total # molecules processed	$(2.7 \pm 0.1) \times 10^{17}$
[b]Dose per molecule, D	39 ± 2 eV

Notes.
[a] Nominal input parameters.
[b] Based on calculations of CASINO output values or known physical parameters.
[c] Obtained from CASINO calculations.
Reference. (*a*) Lewis (1992).

Figure 1. Infrared reflection spectrum of magnesium perchlorate hexahydrate (Mg(ClO$_4$)$_2$·6H$_2$O) within the simulation chamber recorded before irradiation. The temperature of the sample (160 K, 210 K, or 260 K) had no effect on the pre-irradiated spectrum.

system prior to irradiation is shown in Figure 1; mode assignments taken from the literature are listed in Table 2 and agree nicely with our experimental data. At all temperatures, the response of the magnesium perchlorate hexahydrate system during the exposure to energetic electrons is dictated by the decrease in the fundamentals (ν_3, 1184 cm^{-1}; ν_1, 964 cm^{-1}; ν_4, 630 cm^{-1}) and overtone ($2\nu_4$, 1299 cm^{-1}) associated with the perchlorate ion (ClO$_4^-$) (Figure 2). Considering the diffuse reflectance of the samples and hence the limited signal-to-noise ratio of the infrared spectra, it was not feasible to explore to what extent the destruction rate depends on the temperature. Simultaneously with the decay of the perchlorate ion, the infrared data suggest emerging absorptions at 1213, 1174, 1119, 671, and 580 cm^{-1}. A comparison of these positions with data from the literature suggests that these bands can be connected to the formation of the chlorate ion (ClO$_3^-$) during the irradiation and in particular with the overtones ($2\nu_2$, $2\nu_4$), the combination band ($\nu_2 + \nu_4$), and the fundamentals (ν_2, ν_4) (Table 2). Therefore, the infrared data alone provide compelling evidence that perchlorate ions (ClO$_4^-$) are converted to chlorate ions (ClO$_3^-$). Considering the stoichiometry, atomic oxygen (O) is proposed to be the counter fragment of the perchlorate radiolysis. We would like to stress that although our system also contains crystal water (Table 2), no traces of hydrogen peroxide (H$_2$O$_2$)—a common radiolysis product of water ices (H$_2$O) (Zheng et al. 2007a, 2007b, 2009)—could be observed. Moreover, we attribute the increase in the ν_2 fundamental of water (1638 cm^{-1}) to changes in absorption coefficients brought about by lattice alterations during irradiation (Bennett et al. 2014).

3.2. Mass Spectrometry

During the irradiation and warm-up phase, we also probed the species released into the gas phase via a QMS. At all temperatures, this approach only detected a signal at mass-to-charge ratios of $m/z = 16$ and $m/z = 32$, which could be attributed to atomic (O) and molecular oxygen (O$_2$), respectively (Figure 3); the two profiles overlap, suggesting that the signal at $m/z = 16$ originates from dissociative fragmentation of molecular oxygen by the 90 eV electrons in the ionizer of the mass spectrometer. Further, within the detection limits of our
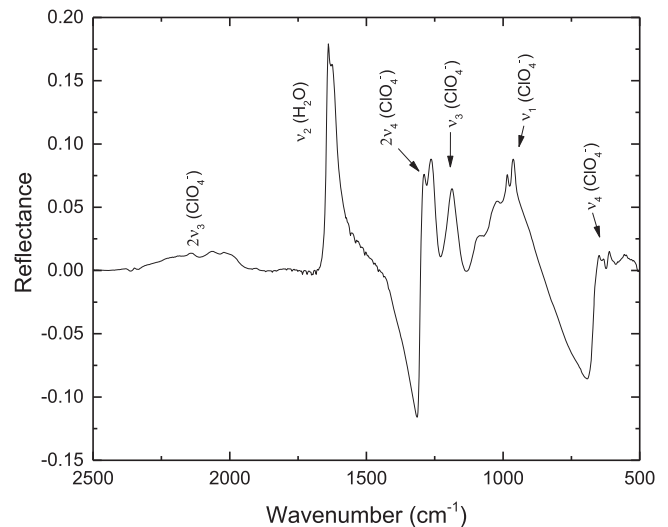
system, neither molecular hydrogen (H$_2$), ozone (O$_3$), hydrogen peroxide (H$_2$O$_2$)—typical degradation products from water (Zheng et al. 2006a, 2006b, 2007b)—nor chlorine-bearing species such as chlorine monoxide (ClO) and chlorine dioxide (ClO$_2$) were observed. Since molecular hydrogen represents a significant residual gas (from outgassing of stainless steel) we also exposed deuterated magnesium perchlorate hexahydrate (Mg(ClO$_4$)$_2$·6D$_2$O) to energetic electrons in an attempt to detect molecular deuterium (D$_2$; $m/z = 4$). However, no signal at $m/z = 4$ could be observed. Also, no signal at $m/z = 36$ (D$_2$O$_2$) was identified; only ion counts at $m/z = 16$ and $m/z = 32$ connected to atomic (O) and molecular oxygen (O$_2$) were observed. Quantitatively speaking, even if D2-hydrogen peroxide (D$_2$O$_2$) is formed, its yields must be at least three orders of magnitude less than those of molecular oxygen. Finally, we irradiated samples of ^{18}O-labeled magnesium perchlorate hexahydrate (Mg(ClO$_4$)$_2$·6H$_2^{18}$O) to elucidate whether the oxygen is released from the water (H$_2^{18}$O) and/or from the perchlorate ions (ClO$_4^-$). Once again, for all temperatures, we only detected a signal at $m/z = 16$ and $m/z = 32$, which could be attributed to atomic (O) and molecular oxygen (O$_2$). No traces of $m/z = 18$ (^{18}O), 34 (^{18}OO), nor 36 (^{18}O$_2$) could be observed. These findings have two key consequences. First, during the irradiation of magnesium perchlorate hexahydrate, the water of hydration stays intact and is not radiolyzed. Second, the oxygen originates solely from the perchlorate ions (ClO$_4^-$) and not from the water of hydration.

Let us have a closer look at the temporal profiles of the signal at $m/z = 32$ associated with the formation of molecular oxygen (O$_2$) recorded at sample temperatures of 260, 210, and 160 K (Figure 3). First, at 260 K, a signal at $m/z = 32$ could be detected with the onset of the electron exposure. At lower temperatures of 210 and 160 K, a delayed release of molecular oxygen from the solid sample into the gas phase is prominent. This delay is more pronounced at 160 K than at 210 K, which suggests a temperature-dependent component of the reaction mechanism—possibly diffusion-limited pathways of the recombination of atomic oxygen to form molecular oxygen

Table 2
Infrared Assignments of Magnesium Perchlorate Hexahydrate (Mg(ClO$_4$)$_2$·6H$_2$O) Before and After Irradiation with 5 keV Electrons.
These Results are Seen for Irradiations at 160, 210, and 260 K

Literature (cm^{-1})	Before Irradiation (cm^{-1})	After Irradiation (cm^{-1})	Carrier	Assignment	References
5102	5217	...	$\nu_2 + \nu_3$(H$_2$O)	Combination	(1)
4150	4188	...	(H$_2$O)	...[a]	(2)
3610	3633	...	ν_3(H$_2$O)	OH asymmetric stretch	(2)
3221	3222	...	ν_1(H$_2$O)	OH symmetric stretch	(1)
2230	2144	...	$2\nu_3$(ClO$_4^-$)	Overtone	(1)–(3)
1650	1638	...	ν_2(H$_2$O)	OH bend	(1), (2)
1250	1299	...	$2\nu_4$(ClO$_4^-$)	Overtone	(1), (3)
1234	...	1213	$2\nu_2$(ClO$_3^-$)	Overtone	(1), (4)
1161	1184	...	ν_3(ClO$_4^-$)	Symmetric stretch	(4)
1132	...	1174	$2\nu_4$(ClO$_3^-$)	Overtone	(1), (4)
1110	...	1119	$\nu_2 + \nu_4$(ClO$_3^-$)	Combination	(1)
940	964	...	ν_1(ClO$_4^-$)	Symmetric stretch	(1), (3), (5)
617	...	671	ν_2(ClO$_3^-$)	Symmetric bend	(1)
625	630	...	ν_4 (ClO$_4^-$)	Asymmetric bend	(1), (3)
566	...	580	ν_4(ClO$_3^-$)	Deformation	(1), (4)

Note.
[a] Overtones or combinations of H$_2$O vibrations in a constrained structure.
References. (1) Hanley et al. (2015), (2) Bishop et al. (2014), (3) Chen et al. (2004), (4) Kopitzky et al. (2002), (5) Lutz & Haeuseler (1999).
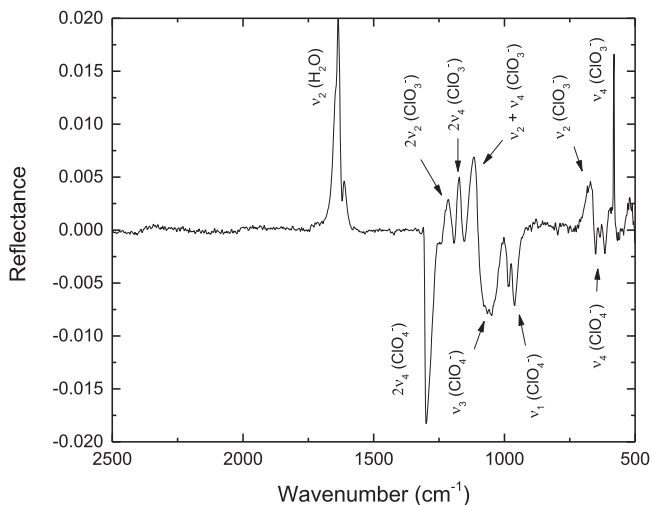
Figure 2. Difference spectrum of the infrared reflectance spectrum of magnesium perchlorate hexahydrate (Mg(ClO$_4$)$_2$·6H$_2$O) before and after the irradiation at 160 K, indicating a loss of perchlorate ions (ClO$_4^-$) and the production of chlorate ions (ClO$_3^-$) and crystalline water. These results are consistent with spectra at 210 and 260 K.

(see Section 4). Once the irradiated sample is warmed up to 300 K, it is evident that the radiolyzed magnesium perchlorate hexahydrate (Mg(ClO$_4$)$_2$·6H$_2$O) still stores molecular oxygen. As the temperature is increased from 160 K/210 K/260 K to 300 K, those oxygen molecules still trapped within the samples sublime, as is evident from an increase in the signal at $m/z = 32$. Since all samples were exposed to identical doses of 39 ± 2 eV and the mass spectrometer was operated at identical settings such as emission current, electron energy, and secondary electron multiplier voltage, we can directly integrate the ion signal at $m/z = 32$ to gain quantitative information (Table 3).

An integration of the ion signal during the warm-up phase suggested that the lower the sample temperature is, the more molecular oxygen that can be stored in the irradiated samples.

This is obvious from the decrease in the integrated ion signal from (5.7 ± 0.6) × 10^{-6} A s (160 K) via (3.2 ± 0.3) × 10^{-6} A s (210 K) to (1.4 ± 0.1) × 10^{-6} A s (260 K). Likewise, a comparison of the total ion current of all oxygen molecules released during the irradiation and in the warm-up phase strongly suggests that the radiolytic yields of molecular oxygen decrease as the sample temperature increases from 160 to 260 K. This is evident from the decrease in the total integrated ion counts of $m/z = 32$ collected during the experiments from (6.2 ± 0.6) × 10^{-6} A s (160 K) via (3.7 ± 0.4) × 10^{-6} A s (210 K) to (3.4 ± 0.3) × 10^{-6} A s (260 K). The diminished yield of radiolytic products during electron irradiation of low-temperature samples has been well documented in the case of, for example, ices of ethane (C$_2$H$_6$, Kim et al. 2010), water (H$_2$O, Moore & Hudson 2000; Baragiola et al. 2003; Orlando & Sieger 2003; Zheng et al. 2006a, 2007b), and ammonia (NH$_3$, Zheng et al. 2008; Zheng & Kaiser 2010) and has been linked to an equilibrium between radiolytic degradation of the molecules in the ices and re-formation of the latter in diffusion-controlled reactions. Since our mass spectrometer is calibrated (Zheng et al. 2006a, 2006b; Turner et al. 2015), it is also feasible to compute the absolute numbers of oxygen molecules formed in the experiments to be (4.4 ± 0.9) × 10^{16} (160 K), (2.6 ± 0.5) × 10^{16} (210 K), and (2.4 ± 0.5) × 10^{16} (260 K), i.e., an overall decrease in the yield of released oxygen molecules, n, as the temperature, T, rises; when this is fit with an exponential curve it gives (Table 3; Figure 4)

$$n = 1.08 \, e^{-0.00606T}. \tag{1}$$

4. DISCUSSION

Before we place the results into the astrophysical context of Mars exploration, we would like to compile first the key results of the experimental studies:

– The infrared data suggest that the response of the perchlorates to the energetic electrons is dictated by the
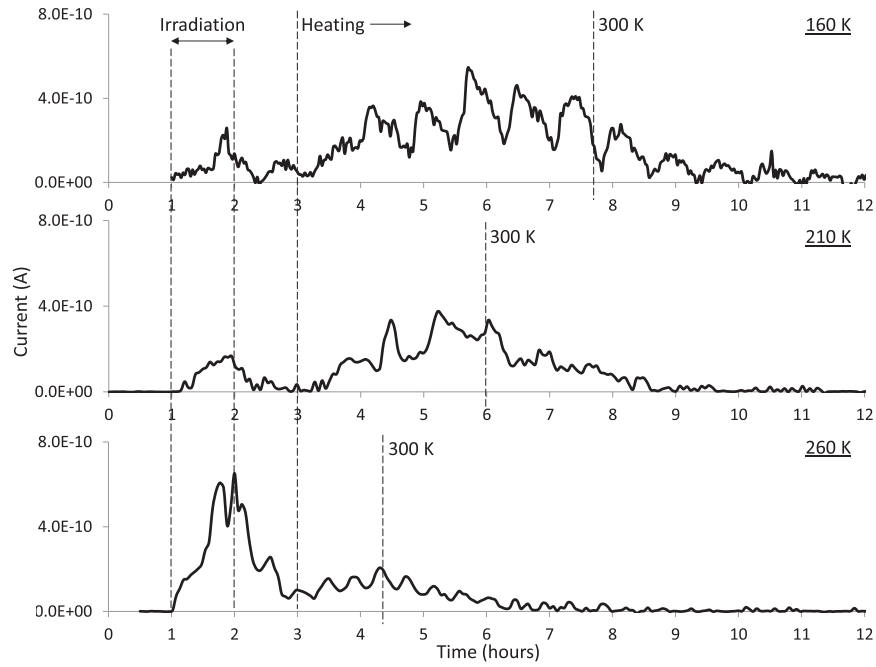
Figure 3. Quadrupole mass spectrometry (QMS) data for $m/z = 32$ (O_2^+) monitoring the release of molecular oxygen during the irradiation of magnesium perchlorate hexahydrate ($Mg(ClO_4)_2 \cdot 6H_2O$) and the heating period to 300 K for three distinct target temperatures. These plots were integrated to determine the total amount of O_2 released (Table 3, Figure 4). The periodic nature of the signal is an instrumental artifact related to fluctuations with the filament.

destruction of the perchlorate ion (ClO_4^-) and the inherent formation of chlorates (ClO_3^-) plus atomic oxygen (O).

– The mass spectrometer detects only molecular oxygen (O_2) and no atomic oxygen (O). Isotopic substitution experiments reveal that the oxygen is released solely from the perchlorate ion (ClO_4^-) and not from the water of hydration (H_2O). The overall yield of molecular oxygen increases as the temperature drops from 260 to 160 K.

– During the irradiation of the samples, the emission of molecular oxygen from the samples is delayed with respect to the onset of irradiation. This time delay becomes more pronounced as the temperature drops from 260 to 160 K. It is likely an effect of a required diffusion of the atomic oxygen and recombination to molecular oxygen along with a diffusion of the molecular oxygen outside the irradiated sample.

We would like to discuss now the underlying energetics of the reactions. Considering that the response of the perchlorates (ClO_4^-) to energetic electrons is dictated by the formation of chlorates (ClO_3^-) plus atomic oxygen (O), Equation (2) holds. For the formally spin-allowed reaction, the rupture of the oxygen–chlorine bond to form electronically excited oxygen atoms $O(^1D)$ requires 3.78 eV; on the other hand, the formation of ground-state oxygen $O(^3P)$, which is formally spin-forbidden, requires only 1.81 eV (Johnson 2015). Once released, the oxygen atoms are stored in the solids and/or can diffuse as they eventually recombine via a barrier-less atom–atom reaction, forming molecular oxygen. Note that the lifetime of electronically excited oxygen atoms $O(^1D)$ is of the order of 150 s in the gas phase (Warneck 2000). Therefore, all excited oxygen atoms decay to the $O(^3P)$ electronic ground state during the irradiation or the isothermal phase after the irradiation before the system is warmed up to 300 K.

$$ClO_4^- \rightarrow ClO_3^- + O(^1D) \qquad (2a)$$

$$ClO_4^- \rightarrow ClO_3^- + O(^3P). \qquad (2b)$$
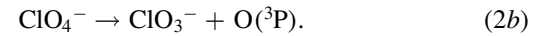
Considering that between 2.4×10^{16} (260 K) and 4.4×10^{16} (160 K) oxygen molecules are formed (Table 3), twice as many perchlorate anions have to be destroyed since one perchlorate anion produces only one oxygen atom, i.e., 4.8×10^{16} (260 K) and 8.8×10^{16} (160 K) perchlorate anions. Accounting for the irradiation area, the density of the samples, and the average penetration depth of the energetic electrons (Table 1), a total of $(5.4 \pm 0.2) \times 10^{17}$ perchlorate ions are exposed, and the data derived from the mass spectrometric analysis suggest that between $(9 \pm 2)\%$ (260 K) and $(16 \pm 4)\%$ (160 K) of the exposed perchlorate ions were destroyed. Accounting for the energy required to cleave the chlorine–oxygen bonds at 160 K, the formation of $(4.4 \pm 0.9) \times 10^{16}$ oxygen molecules requires $(8.8 \pm 1.8) \times 10^{16}$ chlorine–oxygen bond rupture processes and hence a total energy of $(3.3 \pm 0.7) \times 10^{17}$ and $(1.6 \pm 0.3) \times 10^{17}$ eV to generate the oxygen atoms in their ^1D and ^3P states, respectively. These energies are reduced for 260 K to $(1.9 \pm 0.4) \times 10^{17}$ and $(0.9 \pm 0.2) \times 10^{17}$ eV to generate the oxygen atoms in their ^1D and ^3P states, respectively. Taking into account that a total of $(1.1 \pm 0.3) \times 10^{19}$ eV is being transmitted from the impinging electrons to the samples, the energetic considerations propose that, at 160 K, $(3.0 \pm 1.5)\%$ and $(1.5 \pm 0.8)\%$ of the total energy is required to release the oxygen atoms in their ^1D and ^3P states, respectively. As the temperature increases to 260 K, these values drop to $(1.7 \pm 0.8)\%$ and $(0.8 \pm 0.4)\%$ for ^1D and ^3P. In summary, our experiments provide compelling evidence that the degradation of perchlorates (ClO_4^-) by secondary electrons as generated in the track of galactic cosmic rays leads initially to the formation of the chlorate anions (ClO_3^-) along with ground- and/or excited-state *oxygen atoms* (O). The delayed

Table 3
Number of Oxygen Molecules Released During Irradiation and Heating

Initial Temperature (K)	O$_2$ Released During Irradiation (molecules)	O$_2$ Released During Heating (molecules)	Total O$_2$ Released (molecules)
160	$(3.9 \pm 0.8) \times 10^{15}$	$(4.1 \pm 0.8) \times 10^{16}$	$(4.4 \pm 0.9) \times 10^{16}$
210	$(3.4 \pm 0.7) \times 10^{15}$	$(2.3 \pm 0.5) \times 10^{16}$	$(2.6 \pm 0.5) \times 10^{16}$
260	$(1.4 \pm 0.3) \times 10^{16}$	$(1.0 \pm 0.2) \times 10^{16}$	$(2.4 \pm 0.5) \times 10^{16}$

Note. This table shows the number of oxygen molecules (O$_2$) released during the irradiation of magnesium perchlorate hexahydrate (Mg(ClO$_4$)$_2$·6H$_2$O) and heating to 300 K. These numbers were obtained by integrating the mass spectrometric signal at $m/z = 32$ (Figure 3) and using conversion factors obtained from calibrated experiments
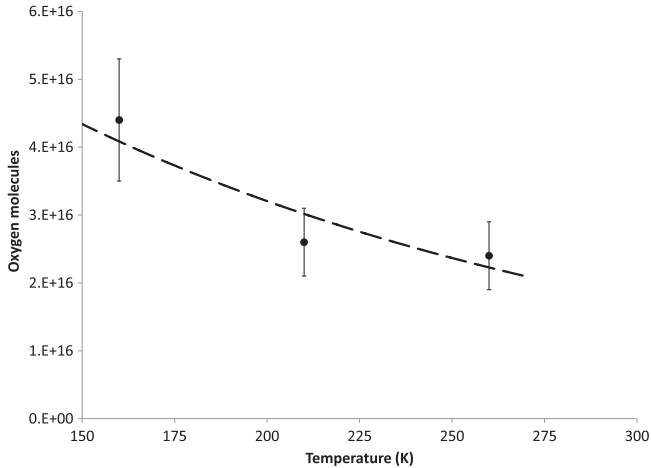
Figure 4. Total number of oxygen molecules (O$_2$) formed during the radiation exposure of magnesium perchlorate hexahydrate (Mg(ClO$_4$)$_2$·6H$_2$O). The dashed line represents the temperature-dependent fit of the data and shows that more oxygen molecules formed at lower temperatures.

emission and eventual mass spectrometric detection of *molecular oxygen* (O$_2$) strongly indicates a diffusion-limited component of the reaction mechanism when the (thermalized) oxygen atoms recombine and also when the molecular oxygen diffuses out of the perchlorate samples. Quantitatively speaking, approximately 16% of the perchlorates can be degraded to eventually yield molecular oxygen at radiation doses of 39 ± 2 eV per perchlorate unit.

We would like to discuss our findings in the context of previous experiments on the degradation of perchlorates by ionizing radiation. Similar to our results, Bugaenko (1970) and Wang et al. (1966) concluded that the chlorate anion (ClO$_3^-$) represents the main product of the ^{60}Co γ-exposed aqueous solutions of perchlorates in the temperature range from 293 K to 77 K; chlorite (ClO$_2^-$), hypochlorite (ClO$^-$), and chloride (Cl$^-$) were proposed as higher order reaction products formed via the degradation of the chlorate anion. Likewise, the radiolysis of solid ammonium perchlorates at 293 K with less than 0.18 MeV X-rays yielded chlorates as the primary product (Nevostruev et al. 1969). Shimokoshi et al. exploited electron paramagnetic resonance (EPR) spectroscopy to detect the related chlorine trioxide (ClO$_3$) radical in ^{60}Co γ-radiolyzed magnesium perchlorate (Mg(ClO$_4$)$_2$) samples at temperatures below 193 K (Shimokoshi & Mori 1973). Prince et al. also probed the ^{60}Co γ-induced decomposition of perchlorates at 193 K (Prince & Johnson 1965). Their findings revealed that the chlorate ion represents the dominant radiolysis product, accounting for up to 92% of all newly formed chlorine-bearing molecules with yields of 4.3×10^{-2} ions eV^{-1}. Finally, Hart

& Brown (1980) investigated the yields of ground-state oxygen (O(^{3}P))—and based on the stoichiometry the yields of chlorates —of ^{60}Co γ-radiolyzed (1.17 and 1.33 MeV) aqueous perchlorate solutions at 293 K, revealing atomic oxygen yields of 2.8×10^{-3} atoms eV^{-1}. Although different irradiation sources were exploited (^{60}Co γ rays versus energetic electrons), this value has a similar order of magnitude to our chlorate yields, ranging from $(8.0 \pm 2.5) \times 10^{-3}$ ions eV^{-1} (160 K) to $(4.6 \pm 1.5) \times 10^{-3}$ ions eV^{-1} (260 K). Further, Quinn et al. (2011) reported the processing of Mg(ClO$_4$)$_2$ with 1.487 keV X-rays. However, no irradiation dose was provided, nor was a description of sample preparation, making quantitative comparison of the present experiment not possible. Their findings include the formation of ClO$_3^-$, ClO$_2^-$, ClO$^-$, and Cl$^-$ after 99% of the magnesium perchlorate had been decomposed, and the detection of molecular oxygen (O$_2$) after humidifying their sample, showing that further processing was necessary to detect O$_2$. However, the detection of O$_2$ in the present experiment was during the irradiation phase as well as during the heating and did not require any further processing.

5. ASTROPHYSICAL IMPLICATIONS

Our experiments demonstrated nicely that the degradation of magnesium perchlorate hexahydrate (Mg(ClO$_4$)$_2$·6H$_2$O) by energetic electrons at temperatures between 160 K and 260 K leads initially to the formation of chlorate anions (ClO$_3^-$) along with atomic oxygen (O); within the perchlorate minerals, the oxygen atoms can diffuse and recombine to form molecular oxygen (O$_2$), which is eventually released into the gas phase as detected by a mass spectrometer. The investigations revealed further that the yields of molecular oxygen are strongly temperature-dependent and rise as the temperature drops from 260 to 160 K from $(2.4 \pm 0.5) \times 10^{16}$ to $(4.4 \pm 0.9) \times 10^{16}$ oxygen molecules at a dose of 39 ± 2 eV per perchlorate unit. This translates into destruction rates of the perchlorate anions as high as $(16 \pm 5)\%$ with between $(3.0 \pm 1.5)\%$ and $(1.5 \pm 0.8)\%$ of the total energy of the impinging radiation converted into the release of the oxygen atoms in their ^{1}D and ^{3}P states (160 K); as the temperature increases to 260 K, these fractions decrease to $(1.7 \pm 0.8)\%$ and $(0.8 \pm 0.4)\%$ for ^{1}D and ^{3}P, respectively. It is crucial to transfer these laboratory findings to the real planetary surface settings. Therefore, our experiments reveal that atomic as well as molecular oxygen, which is formed via recombination of atomic oxygen as released from the perchlorate ions by exposure to ionizing radiation, but not from the water of hydration, represent the oxidizing species capable of reacting with organic molecules in the Martian regolith. It should be stressed that, in our laboratory experiment, solely molecular oxygen was detected as a recombination product of atomic oxygen. However, on the Martian surface, the low concentration of perchlorates of only

0.4%–0.6% might also lead to an "isolation" of a perchlorate anion in the neighborhood of an organic molecule. Therefore, the oxygen atom released from the perchlorate via Equation (2) can react with the organic molecule and hence degrade it prior to recombination with a second oxygen atom. The oxidation of organic molecules such as purine nucleobase adenine ($C_5N_5H_5$) via addition of atomic oxygen to the π-electron density and formation of epoxide bonds along with aldehydes has been well demonstrated in laboratory experiments (Evans et al. 2011).

Considering that our experiments exploited energetic electrons, thus mimicking secondary electrons generated in the track of galactic cosmic rays (Molina-Cuberos et al. 2001; Dartnell et al. 2007; Pavlov et al. 2012), it is important to provide a quantitative means for the planetary science community to exploit our data in future planetary surface models investigating the degradation of organic compounds in the Martian regolith. Here, our data suggest that from $(8.0 \pm 2.5) \times 10^{-3}$ perchlorate ions (160 K) to $(4.6 \pm 1.5) \times 10^{-3}$ ions (260 K) are degraded per eV. This in turn translates to production rates of molecular oxygen of $(4.0 \pm 1.3) \times 10^{-3}$ molecules eV^{-1} (160 K) to $(2.3 \pm 0.8) \times 10^{-3}$ molecules eV^{-1} (260 K). It is important to stress that the GCRs are distributed isotropically over the Martian surface and have little preference for polar latitudes over equatorial latitudes—unlike Earth—as Mars is a non-magnetic planet for all practical purposes (Cooper et al. 2003, 2006; Schwadron et al. 2012). The remnant crustal magnetic field at Mars, which is much weaker than the global magnetic field of Earth, indicates a magnetic process on ancient Mars. Further, Pavlov et al. (2012) determined a GCR dose accumulation rate of 0.05 J kg^{-1} yr^{-1} at the surface of Mars. As GCRs can penetrate up to two meters below the surface, but the dosage falls off with depth due to absorption, we can consider the top meter of Martian crust with an average dose accumulation rate of 0.03 J kg^{-1} yr^{-1} (Wilson et al. 2016). Assuming a rock density of 2 g cm^{-3}, this would convert to 1.2×10^9 eV cm^{-2} s^{-1} absorbed over 1 m of rock. This approximation assumes that the GCR flux at Mars is the same as at Earth, where the flux is most likely larger due to weaker modulation by the heliosphere at Mars and no Martian magnetic field being present. It also presumes that GCRs are in the energy range from 20 MeV to 10,000 GeV because particles with energies less than 20 MeV would not reach the surface due to heliospheric modulation and the flux of particles with energies exceeding 10,000 GeV is not substantial. Nevertheless, combining these considerations with our production rates of molecular oxygen of $(4.0 \pm 1.3) \times 10^{-3}$ molecules eV^{-1} (160 K) to $(2.3 \pm 0.8) \times 10^{-3}$ molecules eV^{-1} (260 K) provides a good order of magnitude to estimate the production rate of molecular oxygen on the Martian surface within the top meter of soil to be $(4.8 \pm 1.5) \times 10^6$ oxygen molecules cm^{-2} s^{-1}, i.e., $(1.7 \pm 0.6) \times 10^{14}$ oxygen molecules m^{-2} yr^{-1}. Considering the annual influx of about 15 ng of amino acids per m^2 per year (Ten Kate et al. 2005) and assuming for simplicity that these amino acids are solely glycine (NH_2CH_2COOH), this would translate into a flux of 1.2×10^{14} glycine molecules m^{-2} yr^{-1}. Therefore, on average, the majority of the glycine molecules could be oxidized by the molecular oxygen formed in the degradation of the perchlorates. Finally, it is important to consider that the irradiation of the Martian surface by GCRs may not be the only radiolytic source of chlorine oxides in the Mars environment. Pavlov et al. (2012) calculated that during periods of low obliquity on Mars, which is only about 10% of Mars's lifetime when the atmospheric

pressure was 0.2 mbar (Armstrong et al. 2004), the dosage of solar cosmic rays (SCRs) of about 6–0.5 J kg^{-1} yr^{-1} at depths of 0–5 cm can exceed that of GCRs (0.052–0.050 J kg^{-1} yr^{-1}; 0–5 cm; 7 mbar). However, the total accumulation of radiation dose due to SCRs is minor in current Martian atmospheric conditions (7 mbar) when compared to GCRs. Furthermore, the SCR dosage in these periods of low pressure would drop off by two orders of magnitude below the top few centimeters of regolith (Pavlov et al. 2012), making SCR a likely minor radiation source for the degradation of organics below 5 cm.

REFERENCES

Archer, P. D., Franz, H. B., Sutter, B., et al. 2014, JGRE, 119, 237
Armstrong, J. C., Leovy, C. B., & Quinn, T. 2004, Icar, 171, 255
Bada, J. L. 2009, PNAS, 106, E85
Baragiola, R., Vidal, R., Svendsen, W., et al. 2003, NIMPB, 209, 294
Bennett, C. J., Ennis, C. P., & Kaiser, R. I. 2014, ApJ, 782, 63
Bennett, C. J., Jamieson, C., Mebel, A. M., & Kaiser, R. I. 2004, PCCP, 6, 735
Biemann, K. 1979, JMolE, 14, 65
Biemann, K., & Lavoie, J. M. 1979, JGRB, 84, 8385
Biemann, K., Oro, J., Toulmin III, P., et al. 1976, Sci, 194, 72
Biemann, K., Oro, J., Toulmin III, P., et al. 1977, JGR, 82, 4641
Bishop, J. L., Quinn, R., & Dyar, M. D. 2014, AmMin, 99, 1580
Bland, P. A., & Smith, T. B. 2000, Icar, 144, 21
Bugaenko, L. T. 1970, Sovrem Probl Fiz Khim, 14, 156
Callahan, M. P., Smith, K. E., Cleaves II, J. H., et al. 2011, PNAS, 108, 13995
Chen, Y., Zhang, Y.-H., & Zhao, L.-J. 2004, PCCP, 6, 537
Cooper, G. W., & Cronin, J. R. 1995, GeCoA, 59, 1003
Cooper, J. F., Christian, E. R., Richardson, J. D., & Wang, C. 2003, EM&P, 92, 261
Cooper, J. F., Johnson, R. E., Richardson, J. D., & Leblanc, F. 2006, AsBio, 6, 437
Cronin, J., & Chang, S. 1993, in The Chemistry of Life's Origins, ed. J. M. Greenberg, C. X. Mendoza-Gómez, & V. Pirronello (Netherlands: Springer), 209
Dartnell, L. R., Desorgher, L., Ward, J. M., & Coates, A. J. 2007, GeoRL, 34, L02207
Drouin, D., Couture, A. R., Joly, D., et al. 2007, Scanning, 29, 92
Evans, N. L., Bennett, C. J., Ullrich, S., & Kaiser, R. I. 2011, ApJ, 730, 69
Flynn, G. 1996, EM&P, 72, 469
Flynn, G. J., Treiman, A. H., Newsom, H. E., & Farmer, J. D. 1997, in Early Mars: Geologic and Hydrologic Evolution, Physical and Chemical Environments, and the Implications for Life, ed. S. M. Clifford (Houston, TX: Lunar and Planetary Institute), 33
Freissinet, C., Glavin, D. P., Mahaffy, P. R., et al. 2015, JGRE, 120, 495
Glavin, D. P., Freissinent, C., Miller, K. E., et al. 2013, JGRE, 118, 1955
Hanley, J., Chevrier, V. F., Barrows, R. S., Swaffer, C., & Altheide, T. S. 2015, JGRE, 120, 1415
Hart, E. J., & Brown, W. G. 1980, JPhCh, 84, 2237
Hartmann, W. K. 1977, Icar, 31, 260
Hayatsu, R., & Anders, E. 1981, Top Curr. Chem., 99, 1
Hecht, M. H., Kounavles, S. P., Quinn, R. C., et al. 2009, Sci, 325, 64
Hintze, P. E., Buhler, C. R., Schuerger, A. C., Calle, L. M., & Calle, C. I. 2010, Icar, 208, 749
Hovington, P., Drouin, D., & Gauvin, R. 1997, Scanning, 19, 1
Johnson, R. D., III 2015, NIST Computational Chemistry Comparison and Benchmark Database, NIST Standard Reference Database Number 101, Release 17b, http://cccbdb.nist.gov/
Jungclaus, G. A., Yuen, G. U., Moore, C. B., & Lawless, J. G. 1976, Metic, 11, 231
Kim, Y. S., Bennett, C. J., Li-Hsieh, C., Brien, K. O., & Kaiser, R. I. 2010, ApJ, 711, 744
Kim, Y. S., Wo, K. P., Maity, S., Atreya, S. K., & Kaiser, R. I. 2013, JAChS, 135, 4910
Kopitzky, R., Grothe, H., & Willner, H. 2002, CEJ, 8, 5601
Kounaves, S. P., Carrier, B. L., O'Neil, G. D., Stroble, S. T., & Claire, M. W. 2014a, Icar, 229, 206

Kounaves, S. P., Chaniotakis, N. A., Chevrier, V. F., et al. 2014b, Icar, 232, 226
Kounaves, S. P., Hecht, M. H., Kapit, J., et al. 2010, JGRE, 115, E00E10
Lewis, R. J. 1992, Hawley's Condensed Chemical Dictionary (12th ed.; New York: Van Nostrand Reinhold)
Lutz, H., & Haeuseler, H. 1999, JMoSt, 511, 69
Marcus, A. H. 1968, Sci, 160, 1333
Martins, Z., Botta, O., Fogel, M., et al. 2008, E&PSL, 270, 130
McKay, C. P., Grunthaner, F. J., Lane, A. L., et al. 1998, P&SS, 46, 769
Ming, D. W., Archer Jr., P. D., Glavin, D. P., et al. 2014, Sci, 343, 1245267
Ming, D. W., Lauer Jr., H. V., Archer Jr., P. D., et al. 2009, in 40th Lunar and Planetary Science Conf., Combustion of Organic Molecules by the Thermal Decomposition of Perchlorate Salts: Implications for Organics at the Mars Phoenix Scout Landing Site (The Woodlands, TX: Lunar and Planetary Institute), 2241
Molina-Cuberos, G. J., Stumptner, W., Lammer, H., Kömle, N. I., & O'Brien, K. 2001, Icar, 154, 216
Moore, M., & Hudson, R. 2000, Icar, 145, 282
Navarro-González, R., Vargas, E., de la Rosa, J., Raga, A. C., & McKay, C. P. 2010, JGRE, 115, E12010
Nevostruev, V. A., Zakharov, Y. A., & Anikeeva, V. V. 1969, Izv Tomsk Politekh Inst, 199, 80
Noblet, A., Stalport, F., Guan, Y. Y., et al. 2012, AsBio, 12, 436
Orlando, T., & Sieger, M. 2003, SurSc, 528, 1
Oró, J., Gibert, J., Lichtenstein, H., Wikstrom, S., & Flory, D. A. 1971, Natur, 230, 105
Oró, J., & Holzer, G. 1979, JMolE, 14, 153
Pang, K. D., Chun, S. F. S., Ajello, J. M., Nansheng, Z., & Minji, L. 1982, Natur, 295, 43
Pavlov, A. A., Vasilyev, G., Ostryakov, V. M., Pavlov, A. K., & Mahaffy, P. 2012, GeoRL, 39, L13202
Peeters, Z., Botta, O., Charnley, S. B., Ruiterkamp, R., & Ehrenfreund, P. 2003, ApJL, 593, L129

Pering, K. L., & Ponnamperuma, C. 1971, Sci, 173, 237
Prince, L. A., & Johnson, E. R. 1965, JPhCh, 69, 359
Quinn, R., Grunthaner, P., Taylor, C., Bryson, C., & Grunthaner, F. 2011, LPSC, 42, 2003
Quirico, E., Borg, J., Raynal, P.-I., Montagnac, G., & d'Hendecourt, L. 2005, P&SS, 53, 1443
Schwadron, N. A., Baker, T., Blake, B., et al. 2012, JGRE, 117, E00H13
Shimokoshi, K., & Mori, Y. 1973, JPhCh, 77, 3058
Smith, M. L., Claire, M. W., Catling, D. C., & Zahnle, K. J. 2014, Icar, 231, 51
Stalport, F., Coll, P., Szopa, C., Cottin, H., & Raulin, F. 2009, AsBio, 9, 543
Sutter, B., Archer, D., Ming, D. W., et al. 2013, Lunar Planet Sci, 44, 2046
Sutter, B., Ming, D. W., Boynton, W. V., et al. 2009, The New Martian Chemistry Workshop, Summary of Results from the Mars Phoenix Lander's Thermal Evolved Gas Analyzer (Medford, MA: Lunar and Planetary Institute), 8004
Ten Kate, I. L., Garry, J. R. C., Peeters, Z., et al. 2005, M&PS, 40, 1185
Ten Kate, I. L., Garry, J. R. C., Peeters, Z., Foing, B., & Ehrenfreund, P. 2006, P&SS, 54, 296
Turner, A. M., Abplanalp, M. J., Chen, S. Y., et al. 2015, PCCP, 17, 27281
Wang, W.-H., Bugaenko, L. T., & Belevskii, V. N. 1966, Zh Fiz Khim, 40, 2764
Warneck, P. 2000, Chemistry of the Natural Atmosphere (2nd ed.; San Diego: Academic)
Werner, S. C. 2008, Icar, 195, 45
Wilson, E. H., Atreya, S. K., & Kaiser, R. I. 2016, JGR, submitted
Yuen, G., Blair, N., Des Marais, D. J., & Chang, S. 1984, Natur, 307, 252
Zheng, W., Jewitt, D., & Kaiser, R. I. 2006a, ApJ, 639, 534
Zheng, W., Jewitt, D., & Kaiser, R. I. 2006b, ApJ, 648, 753
Zheng, W., Jewitt, D., & Kaiser, R. I. 2007a, PCCP, 9, 2556
Zheng, W., Jewitt, D., & Kaiser, R. I. 2007b, ChPhL, 435, 289
Zheng, W., Jewitt, D., Osamura, Y., & Kaiser, R. I. 2008, ApJ, 674, 1242
Zheng, W. J., Jewitt, D., & Kaiser, R. I. 2009, JPCA, 113, 11174
Zheng, W. J., & Kaiser, R. I. 2010, JPCA, 114, 5251